A Comparative Study on the Condensation Heat Transfer of R-513A as an Alternative to R-134a

Andreas Karageorgis [1], George Hinopoulos [1] and Man-Hoe Kim [2],*

[1]   Halcor-Copper Tube Division, ElvalHalcor Company, 32011 Oinofyta, Viotia, Greece;
      akarage@halcor.com (A.K.); ghinopoulos@halcor.com (G.H.)
[2]   School of Mechanical Engineering & IEDT, Kyungpook National University, Daegu 41566, Korea
*   Correspondence: manhoe.kim@knu.ac.kr; Tel.: +82-53-950-5576; Fax: +82-53-950-6500

Abstract: This paper presents the two-phase condensation heat transfer and pressure drop characteristics of R-513A as an alternative refrigerant to R-134a in a 9.52-mm OD horizontal microfin copper tube. The test facility had a straight, horizontal test section with an active length of 2.0 m and was cooled by cold water circulated in a surrounding annular space. The annular-side heat transfer coefficients were obtained using the Wilson plot method. The average heat transfer coefficient and pressure drop data are presented at the condensation temperature of 35 °C in the range of 100–440 $kg \cdot m^{-2} \cdot s^{-1}$ mass flux. The test data of R-513A are compared with those of R-134a, R-1234yf, and R-1234ze(E). The average condensation heat transfer coefficients of the R-513A and R-1234ze(E) refrigerants were similar to R-134a at the lower mass flux (100~150 $kg \cdot m^{-2} \cdot s^{-1}$), while they were up to 10% higher than R-134a as the mass flux increased. The pressure drop of R-513A was similar to R-1234yf and 10% lower than that of R-134a at the higher mass flux. The R-1234ze(E) pressure drops were 20 % higher compared to those of R-134a at the higher mass flux.

Keywords: condensation heat transfer; microfin tube; low-GWP refrigerant; R-513A; R-1234yf; R-1234ze(E)

1. Introduction

In recent years, the use of energy systems, including refrigeration and air-conditioning systems, has been gradually increasing due to the advancement of technology and the improvement of living standards. At the same time, energy supply/demand and environmental problems are emerging as important issues. The environmental impacts of refrigeration and air-conditioning systems and their influence on global warming occur during the generation of the working fluids of the system and because of the power required for operation of the systems.

Global warming is highly affected by air-conditioning, refrigeration, and heat pump systems that account for 700 million metric tons of CO_2-equivalent direct (7~19%) and indirect emissions (74%) per year [1]. Therefore, it is very important to increase the energy efficiency of such systems and to use eco-friendly alternative refrigerants such as carbon dioxide and hydofluoro-olefin (HFO) refrigerants with smaller global warming potentials (GWP) [2–4]. Heat exchangers in air-conditioning and heat pump applications play an important role in the system efficiency and physical size. Finned, round tube, or flat tube heat exchangers are widely used for the evaporators and condensers in residential air-conditioning and heat pump systems.

To investigate the overall performance of the finned-tube heat exchangers, the tube-side heat transfer and pressure drop characteristics as well as airside performance should be investigated simultaneously. Several researchers have conducted investigations into the two-phase thermal and hydraulic performance in smooth and enhanced tubes. Kim and Shin [5,6] experimentally investigated heat transfer characteristics during evaporation and condensation using R-22 and R-410A in 9.52-mm OD smooth and microfin tubes.

They found that the average evaporation and condensation heat transfer coefficients of R-410A for microfin tubes were 1.86~3.27 and 1.7~3.1 times larger than those of smooth tubes, respectively.

They also reported that the evaporation heat transfer coefficients of R-410A were 97–129% of those of R-22 when compared to R-22 under the same test conditions. Due to the EU Regulation No. 517/2014, the refrigerant R-134a is already banned in mobile air-conditioning and household refrigerator-freezer systems and will be also prohibited for commercial refrigerator-freezers from 2022 [7]. Hence, studies to find low-GWP alternative refrigerants for R-134a to prevent negative effects on climate change have attracted the attention of many researchers [8].

Aprea et al. [9] conducted experimental research on energy and environmental analysis of drop-in replacements of R-134a in a household refrigerator. They used R-1234yf and R-1234ze (E) and mixtures with R-134a as drop-in alternatives and reported that both mixtures showed a lower environmental impact compared to R-134a. Yıldız and Yıldırım [10] conducted a theoretical and experimental study on R134a, R1234yf, and R513A refrigerants as working fluids for a heat pump at the evaporator (-10, -5, and $0\,^{\circ}C$) and condenser ($35\,^{\circ}C$) temperatures, and found that R-513A and R-1234yf had lower emissions compared to R-134a.

Table 1 and Figure 1 show the general properties and vapor pressures of R-134a compared to the alternative refrigerants R-1234yf, R-1234ze(E), and R-513A. The GWP values of R-1234yf and R-1234ze(E) were significantly lower than R-134a. The thermo-physical properties of refrigerants in Table 1 and Figure 1 were calculated using NIST REFPROP [11]. However, R-1234yf and R-1234ze(E) are mildly flammable and classified as A2L. R-1234ze(E) has a lower saturation pressure than R-134a (75% of R-134a at a saturation temperature of $35\,^{\circ}C$); therefore, the design of the system requires modification, and the pressure drop is relatively high.

Zhao et al. [12] investigated film condensation heat transfer characteristics on four different single horizontal low-fin tubes using R-134a and R-404A refrigerants. They found that R-404A condensation heat transfer was more sensitive to low-fin configurations and thermal conductivity compared with that of R-134a. Ji et al. [13] conducted an experimental study on the condensation heat transfer of R-134a, R-1234ze(E), and R-290 outside smooth and enhanced titanium tubes at the condensation temperatures of 35 and $40\,^{\circ}C$ in the range of heat flux of 8–80 kW/m^2. The test results indicated that the overall condensation heat transfer coefficients of R-1234ze(E) and R-290 were lower than that of R-134a for both plain and enhanced tubes.

The R-513A refrigerant is an azeotropic mixture with a mass ratio of R-1234yf and R-134a of 56 to 44, and its GWP is slightly higher at 573; however, it is not flammable and has the advantage that it has very similar thermodynamic properties to R-134a. R-513A is used as a short-term replacement of R-134a for retrofit of an existing system. Diani et al. [14–16] performed an experimental study on R-1234yf flow boiling and condensation inside 2.4 and 3.4 mm microfin tubes, respectively.

Table 1. The general properties of R-134a alternative refrigerants [11].

	R-134a	**R-513A**	**R-1234yf**	**R-1234ze(E)**
Chemical formula	CF_3CH_2F	R-1234yf/134a (56/44 wt.%)	CH_2CFCF_3	$C_3H_2F_4$
Molar mass [g/mol]	102	108	114	114
ODP	0	0	0	0
GWP	1430	573	4	6
Flammability	A1	A1	A2L	A2L
NBP [°C]	-26	-29	-29	-19
Tc [°C]	101	96.5	94.7	109.4
Pc [kPa]	4059	3648	3381	3632
q_v * [kJ/m^3]	7293	7373	6891	5608

* Volumetric capacity obtained based on the condensing temperature of $35\,^{\circ}C$.
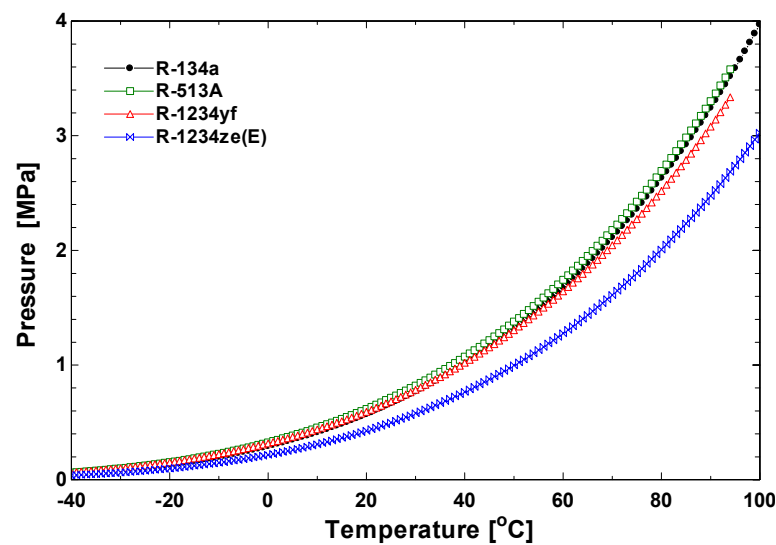
Figure 1. Saturation vapor pressures of R-134a alternative refrigerants [11].

Longo and Zilio [17] investigated the thermal hydraulic characteristics of R-134a and R-1234yf during condensation in a brazed plate heat exchanger. They found that the heat transfer coefficients and pressure drops of R-1234yf were 10~12% and 10~20% lower, respectively, compared with those of R-134a under the same operating conditions. Yang and Nalbandian [18] conducted experimental studies on the condensation heat transfer characteristics of R-1234yf and R-134a refrigerants in small diameter microfin tubes. The inside tube diameter and the length of the tube were 4.0 mm and 600 mm, respectively. Their results showed that the condensation heat transfer characteristics were strongly dependent on the two-phase flow patterns at various flow conditions.

Li and Hrnjak [19] investigated the evaporation heat transfer, pressure drop, and flow patterns of R-1234yf in a microchannel tube. Kedzierski and Gonclalves [20] conducted experimental works of convective condensation heat transfer of R-134a, R-32, R-125, and R-410A in a microfin tube, and developed a single heat transfer correlation using dimensionless parameters.

Diani et al. [21] presented experimental results of the condensation heat transfer of R-1234ze(E) and R-134a refrigerants inside microfin tubes with an inner diameter of 3.4 mm at saturation temperatures of 30 and 40 °C. They analyzed the effects of refrigerant mass flux and vapor quality on the condensation heat transfer, and they found that the higher the vapor quality, the higher the heat transfer coefficients in the annular flow regime. For vapor quality lower than 0.7, the condensation heat transfer coefficients increased with the refrigerant mass flux. They also found that pressure drops of R-1234ze(E) were 30% higher than those of R-134a.

Diani and Rossetto [22] investigated the evaporation heat transfer characteristics of R-513A at the saturation temperature of 20 °C for mass fluxes of 150–800 kg/m^{2}s and heat fluxes of 12–60 kW/m^2 inside a horizontal 3.5-mm ID smooth tube and a 3.4-mm ID microfin tube. They compared the test results with empirical correlation data. Diani et al. [23] investigated the condensation heat transfer of R-513A at the saturation temperatures of 30 and 40 °C in the range of 100~1000 kg·m^{-2}·s^{-1} mass flux inside 3.5-mm ID smooth and microfin tubes. The results showed that the condensation heat transfer coefficients increased with the refrigerant mass flux and vapor quality.

The purpose of this study is to compare the condensation heat transfer characteristics of R-513A in a microfin tube as a drop-in replacement refrigerant for R-134a. Average condensation heat transfer and pressure drop experiments are conducted inside a 9.52-mm OD microfin tube at a condensation temperature of 35 °C in the range of 100~440 kg·m^{-2}·s^{-1} mass flux using R-513A, R-134a, R-1234yf, and R-1234ze(E). The correlation equation of the heat transfer coefficient for the annular space of the test section is obtained using the

Wilson plot method. The condensation test results of the refrigerant R-513A are compared with those of R-134a, R-1234yf, and R-1234ze(E).

2. Experiments

2.1. Experimental Facility

A schematic of the experimental facility is shown in Figure 2. The facility consists of one refrigerant loop and two water loops [24]. The refrigerant loop is designed to measure the mean heat transfer coefficient of refrigerant condensing inside a microfin tube. It is mainly composed of a gear pump, a pre-heater, a test section, a heat exchanger, a receiver tank, and a sub-cooler. Refrigerant in a liquid state is pumped from the bottom of the receiver tank to the pre-heater where it is heated until it reaches a state of superheated vapor. With the pre-heater, it is possible to control the refrigerant superheat when it enters the test section.

The refrigerant enters the test section in superheated vapor state and leaves as a subcooled liquid. The test section with a length of 2 m consists of a simple tube-in-tube counter flow heat exchanger as shown in Figure 2b. The refrigerant inside the inner tube condenses, and the water that flows in the annular duct between the two tubes is heated. Chiller 1 is designed to control the conditions of the water entering the test section. After the test section, the refrigerant enters the heat exchanger as a subcooled liquid. The role of the heat exchanger is to control the refrigerant pressure; this is accomplished by heating or cooling the refrigerant loop with water as a secondary means.

The heating or cooling rates at the heat exchanger are small in order to accomplish a high precision pressure regulation. Chiller 2 controls the water temperature and flow rate at the inlet of the heat exchanger. The receiver tank contains refrigerant in both liquid and vapor states at the bottom and top, respectively. The refrigerant outlet is located on the bottom of the receiver tank so that only liquid refrigerant is pumped.

The refrigerant pump is a positive displacement gear pump with a maximum flow of 100 kg/h liquid refrigerant. Special attention is given to the refrigerant inlet pressure and temperature conditions to ensure that the refrigerant's pressure is higher than its vapor pressure at any point in the pump and to avoid any bubble formation within the pump. For that reason, the refrigerant's pressure and temperature is measured at the suction line to ensure that the refrigerant remains in the liquid state.

The pre-heater is an insulated tank that contains a coil of the main loop refrigerant on the top, electrical resistances on the bottom, and a low-pressure fluid; its role is to heat up the liquid refrigerant to a superheated vapor state. The electrical resistor heaters heat the low-pressure refrigerant that evaporates on the bottom of the tank. Then, low-pressure refrigerant vapor condenses on the surface of the main refrigerant loop coil on the top of the tank.

The test section can be described as a simple tube in a tube heat exchanger. It consists of an inner grooved tube mounted inside an outer shell tube with a diameter of 16 mm, so that the refrigerant flows counter-current through the inner tube with the cooling water around it. Figure 3 shows the tested microfin tube, and it has 60 fins with a fin height (h) of 0.25 mm, an apex angle (Υ) of 30°, helix angle (φ) of 15~30°, ID and OD of 8.92 mm and 9.52 mm, respectively, and bottom wall thickness (t_b) of 0.35 mm. The refrigerant condenses in the test section under fully controlled conditions. The pressure and temperature are measured at the inlet and outlet of the test section using temperature sensors (PT100, RTD sensors) and pressure transducers.
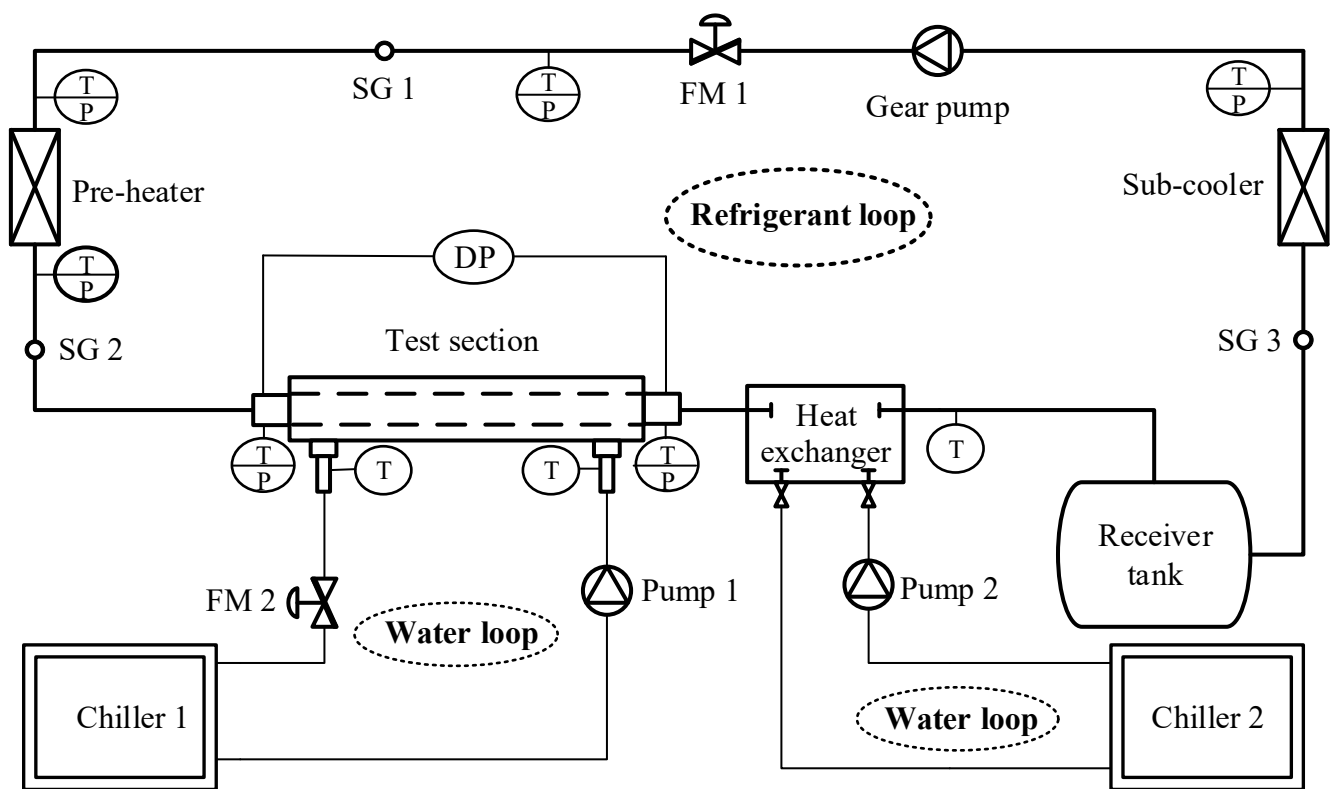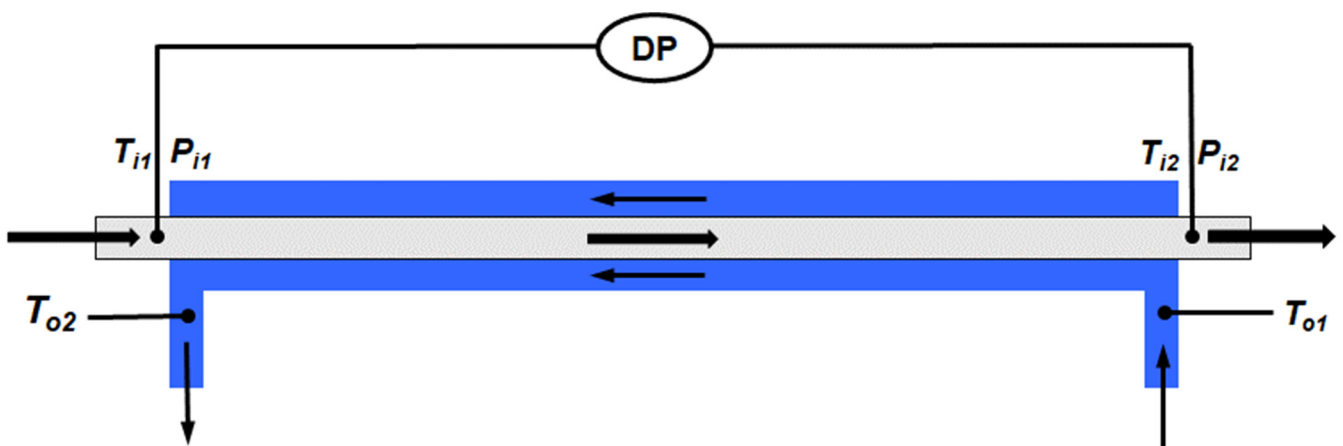
Figure 2. Schematic of the experimental facility (T/P: temperature and pressure sensors, FM: flow meter, DP: differential pressure sensor, and SG: sight glass). (**a**) Instrumentation of the test rig. (**b**) Detailed instrumentation of the test section.
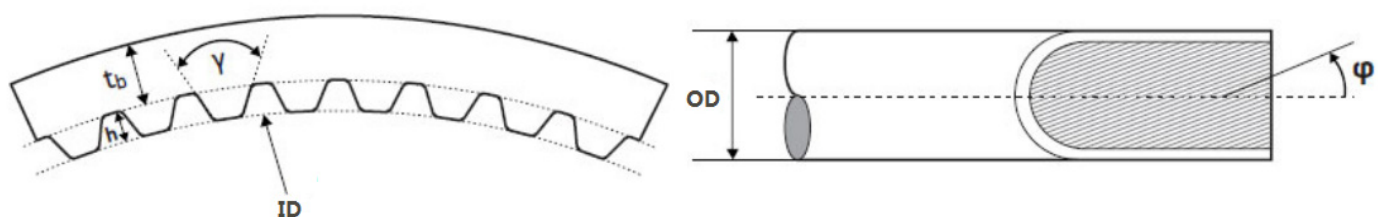

Figure 3. Geometric specification of a tested microfin tube.

The refrigerant pressure drops in the test section are measured with a differential pressure sensor. Both the inlet and outlet state of the refrigerant are single phase; thus, the inlet-outlet specific enthalpies can be determined using thermodynamic data from REFPROP [11]. The measured saturation temperatures were in good agreement with the temperature calculated based on the measured saturation pressure within ±0.3 °C. The condensation heat capacity was calculated as the product of the mass flow and the differential enthalpy. The heat balance between the water and refrigerant side was within the range of ±4.0%. The refrigerant and water flow rates were measured using Coriolis mass flow meters with a nominal flow range of 0~1200 kg/h and an accuracy of ± 0.1%.

The test data were collected using a data recorder and analyzed in real time with a PC running data reduction software. All the information about the test conditions and test data during the experiment were displayed on the monitor, and the test conditions can be changed based on this information.

2.2. Experimental Methods and Conditions

The test conditions are described in Table 2. The condensation experiments were conducted at the saturation temperature of 35 °C for the mass flux of 100~440 kg·m^{-2}·s^{-1} with R-513A, R-134a, R-1234yf, and R-1234ze(E). The inlet superheating and outlet subcooling of condenser were 5 and 2 °C, respectively. The refrigerant flow was regulated by controlling the input power of the variable speed magnetic gear pump. It was not possible to measure the local heat transfer coefficients with variation of quality due to the limitations of the test facility.

Table 2. The test conditions.

Refrigerants	Condensing Temperature [°C]	Mass Flux [kg·m^{-2}·s^{-1}]	Degree of Superheat/ Subcooling [°C]
R-134a, R-513A, R-1234yf, R-1234ze(E)	35	100~440	5/2

Hence, the average condensation heat transfer coefficients and pressure drop data for the refrigerants considered in the study were measured and compared. The test conditions and data to be collected were monitored throughout the experiment, and data sets were recorded and averaged over 10 min after the test conditions reached steady state. Before the condensation experiment, a series of water-to-water experiments were first performed to find the correlation of the heat transfer coefficient of the annular space. The water-to-water test data were collected with increases of the water flow rate of the annular space from 200–800 kg/h in increments of 100 kg/h.

2.3. Data Reduction

The condensation heat transfer coefficients can be calculated using the following equations:

$$\frac{1}{U_o A_o} = \frac{1}{h_i A_i} + R_w + \frac{1}{h_o A_o} \tag{1}$$

where $U_o A_o$ is the overall heat transfer coefficient. The variables h_i and h_o are the refrigerant side and annular waterside heat transfer coefficients. R_w is the thermal conduction resistance of the tube wall, and it can be neglected because the tube material is copper, and the thickness of the tube wall is very thin. The heat transfer rate of the test section, Q, is described using the log mean temperature difference (LMTD):

$$Q = U_o A_o \, LMTD \tag{2}$$

where Q is the arithmetic mean of tube-side (Q_i) and annular-side (Q_o) heat transfer rates that are obtained from the following equations:

$$Q = (Q_i + Q_o)/2 \tag{3}$$

$$Q_i = m_i (e_{i1} - e_{i2}) \tag{4}$$

$$Q_o = m_o c_{po} (T_{o2} - T_{o1}) \tag{5}$$

where m_i and m_o are the refrigerant- and water-side mass flow rates, respectively. e_{i1} and e_{i2}, T_{o1} and T_{o2} are the refrigerant enthalpies and water temperatures at the test section inlet/outlet, respectively. The *LMTD* can be obtained as:

$$LMTD = \frac{(T_{i2} - T_{o1}) - (T_{i1} - T_{o2})}{\ln\left[\frac{(T_{i2} - T_{o1})}{(T_{i1} - T_{o2})}\right]}. \tag{6}$$

If the heat resistance ($1/h_o A_o$) of the annular space is known from Equation (1), the heat transfer coefficient (h_i) in the tube can be obtained from the heat resistance ($1/h_i A_i$) in the tube. The refrigerant properties were calculated using NIST REFPROP [11]. Accounting for all instrument errors, the uncertainties of the average heat transfer coefficient and pressure drop data were $\pm 3.7 \sim 11.3\%$ and $\pm 1.5 \sim 8.5\%$, respectively [25]. The maximum uncertainty for the heat transfer coefficient and pressure drop appeared at the minimum mass flux.

3. Results and Discussion

Figures 4 and 5 show, respectively, the Wilson plot and the correlation equation for obtaining the heat transfer coefficient of the annular space with variation of the water flow rate of 200~800 kg/h. As shown in Figure 4, the total thermal resistance value ($1/U_o A_o$) of the test section was well expressed as a function of the tube-side thermal resistance ($1/h_i A_i$). The total thermal resistance value decreased with the increase of the flow rate of the annular space at the same flow rate in the tube-side because the heat transfer coefficient of the annular flow path increased with the increase of the flow rate. The refrigerant-side heat transfer coefficients were calculated from Equation (1) using the correlation of $1/h_o A_o$ from Figure 5.
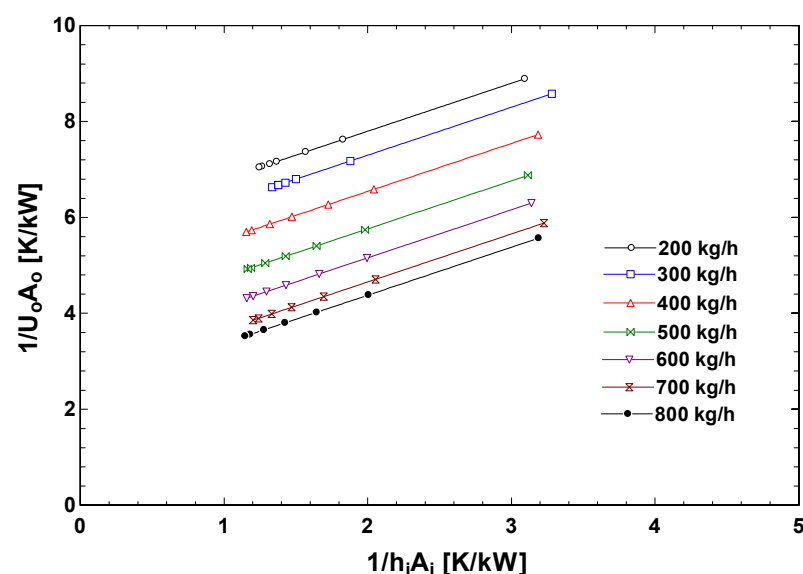

Figure 4. Wilson plots with variation of the annular-side mass flow rate.
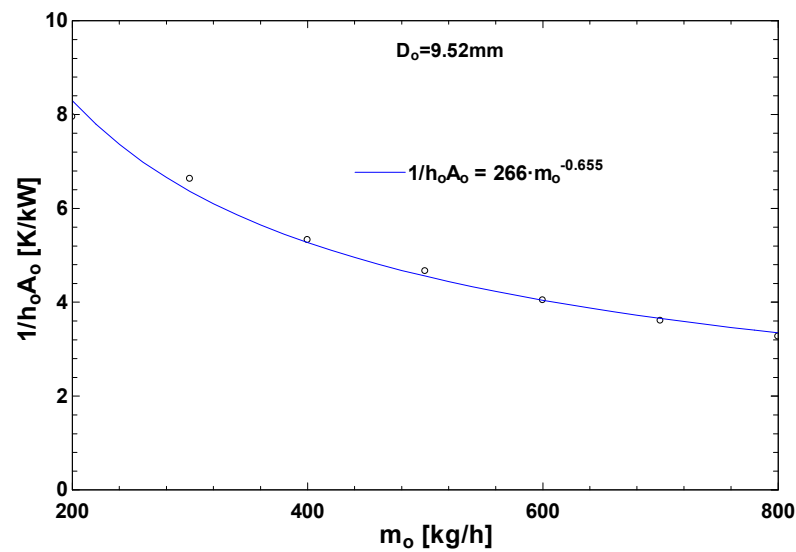
Figure 5. Annular side thermal resistance as a function of the water mass flow rate.

Figures 6 and 7 present the average heat transfer coefficients and pressure drops, respectively, at the condensing temperature of 35 °C in the range of 100~440 kg·m^{-2}·s^{-1} mass flux. The heat transfer coefficients of the test refrigerants, including R-513A, increased with the refrigerant mass flux as expected, and all four refrigerants had similar heat transfer coefficients at low mass flux. However, as the mass flux increased, the heat transfer coefficient of R-513A had a similar value to that of R-1234ze(E), while it was about 10% higher than that of R-134a. The heat transfer coefficient of R-1234yf represents the lowest value among the test refrigerants, and the difference in heat transfer coefficient with other refrigerants became larger as the mass flux increased.
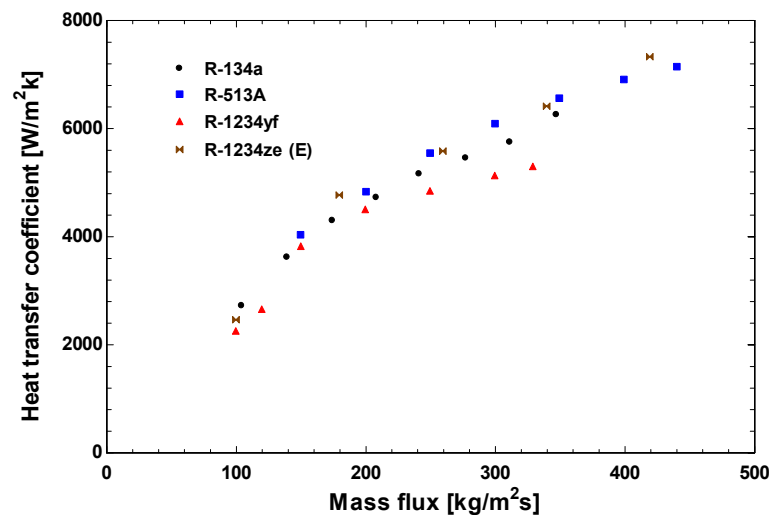

Figure 6. Refrigerant-side heat transfer coefficients with variation of the refrigerant mass flux.
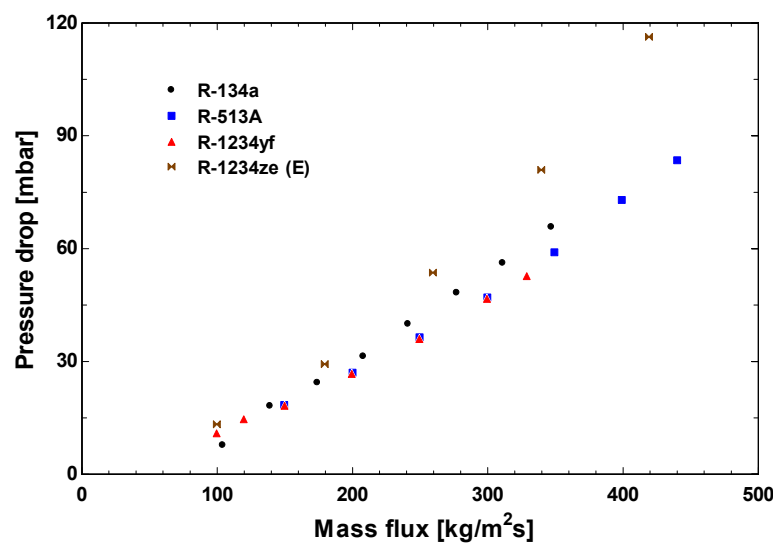
Figure 7. Refrigerant-side pressure drops with variation of the refrigerant mass flux.

The condensation heat transfer coefficient of R-1234yf is up to 12% lower than that of R-134a in the mass flux range probed in this study. Table 3 presents the major thermodynamic and transport properties of R-134a alternative refrigerants. These properties are attributed to the higher R-513A and R-1234ze(E) heat transfer coefficients and lower R-1234yf heat transfer coefficients compared to R-134a. As shown in Figure 7, the pressure drops of all test refrigerants increased with mass flux as expected.

Table 3. The estimated uncertainties.

Parameters	Accuracy/Uncertainty
Temperature	$\pm 0.1\,^{\circ}$C
Pressure	$\pm 0.25\%$
Differential pressure	$\pm 0.1\%$
Mass flow	$\pm 0.1\%$
Average heat transfer coefficient	$\pm 3.7\sim 11.3\%$
Pressure drop	$\pm 1.5\sim 8.5\%$

The pressure drops of R-513A and R-1234yf were smaller than that of R-134a when the mass fluxes were larger than 150 kg·m^{-2}·s^{-1}, while the pressure drops of R-1234ze(E) were relatively higher compared with that of R-134a. The pressure drops of R-513A and R-1234ze(E) were 10% lower and 20% higher than R-134a at the higher mass flux in this study. This is partly due to the higher vapor viscosity of R-1234ze(E) compared to R-134a as shown in Table 4. Overall, R-513A can be used as a short- and mid-term retrofit alternative refrigerant for R-134a due to its relatively good thermo-hydraulic performance and small GWP compared to R-134a.

Table 4. The thermodynamic and transport properties of R-134a alternative refrigerants [11].

Properties [Units]	Refrigerants			
	R-134a	**R-513A**	**R-1234yf**	**R-1234ze(E)**
Saturation temperature [°C]	35	35	35	35
Saturation pressure [kPa]	887	941	895	667
Latent heat [kJ/kg]	168	147	137	159
Liquid viscosity [µPa-s]	172	147	135	168
Vapor viscosity [µPa-s]	12.1	12.0	12.0	12.8
Liquid thermal conductivity [mW/m-K]	76.9	66.3	60.5	70.9
Vapor thermal conductivity [mW/m-K]	14.9	15.1	14.9	14.5
Liquid density [kg/m^3]	1167	1095	1054	1129
Vapor density [kg/m^3]	43.4	50.2	50.3	35.3
Liquid specific heat [J/kg-K]	1471	1464	1443	1422
Vapor specific heat [J/kg-K]	1103	1131	1124	1023
Liquid Prandtl number [-]	3.29	3.23	3.23	3.37
Vapor Prandtl number [-]	0.90	0.90	0.90	0.91
Surface tension [mN/m]	6.74	5.47	4.97	7.56
Reduced pressure [-]	0.18	0.26	0.26	0.18

4. Conclusions

The present study was conducted to investigate two-phase condensation heat transfer and pressure drop characteristics in a horizontal 9.52-mm OD microfin tube with the refrigerant R-513A as an alternative to R-134a. The experimental results of R-513A were compared with those of R-134a, R-1234yf, and R-1234ze. The findings of the present study are as follows:

- The correlation of annular side heat transfer coefficients was obtained as a function of the water mass flow rate and was used to derive the condensation heat transfer coefficients in a microfin tube.
- The average condensation heat transfer coefficients of R-513A and R-1234ze(E) were similar to that of R-134a in the lower range of tested mass fluxes (100~150 kg·m^{-2}·s^{-1}).
- As the mass flux increased, the heat transfer coefficients of R-513A and R-1234ze(E) became up to 10% higher than those of R-134a.
- The average condensation heat transfer coefficients of R-1234yf were up to 12% lower than those of R-134a for the full range of tested mass fluxes.
- The pressure drop of R-513A was similar to R-1234yf and 10% lower compared to that of R-134a at the higher mass flux.
- The R-1234ze(E) pressure drops were 20% higher compared to those of R-134a at the higher mass flux.
- R-513A can be used as a drop-in replacement for R-134a since it has relatively superior condensation heat transfer characteristics and a smaller GWP compared to R-134a.

Author Contributions: Conceptualization, methodology, formal analysis, and original draft preparation by A.K. and G.H., and M.-H.K. supervised the research and edited the manuscript. All authors have read and agreed to the published version of the manuscript.

Institutional Review Board Statement: Not applicable.

Informed Consent Statement: Not applicable.

Data Availability Statement: Data are contained within the article.

Conflicts of Interest: The authors declare no conflict of interest.

Nomenclature

Abbreviations

DP	differential pressure sensor
GWP	global warming potential
HFO	hydofluoro-olefin
ID	inner diameter
FM	flow meter
LMTD	log mean temperature difference
NBP	normal boiling point
OD	outer diameter
ODP	ozone depletion potential
PC	personal computer
SG	sight glass
A	area [m^2]
c_P	specific heat [J/kg-K]
e	enthalpy [J/kg]
h	heat transfer coefficient [W/m^2-K] or fin height [mm]
M	mass flow meter
m	mass flow rate [kg/h]
P	pressure [kPa]
ΔP	pressure drop [mbar]
q_v	volumetric capacity [kJ/m^3]
$\mathcal{Q}$	heat transfer rate [W]
R_w	thermal conduct resistance [K/W]
S	specific entropy [J/kg-K]
T	temperature [°C]
t_b	bottom wall thickness [mm]
U	overall heat transfer coefficient [W/m^2-K]
γ	apex angle [°]
ψ	helix angle [°]

Subscripts

1	inlet
2	outlet
c	critical
i	tube-side
o	annular-side

References

1. Blanco, G.; Gerlagh, R.; Suh, S. (Eds.) Drivers, Trends and Mitigation. In *Climate Change 2014*; Cambridge University Press: Cambridge, UK, 2014; pp. 351–412.
2. Kim, M.-H.; Pettersen, J.; Bullard, C.W. Fundamental Process and System Design Issues in CO_2 Vapor Compression Systems. *Prog. Energy Combust. Sci.* **2004**, *30*, 119–174. [CrossRef]
3. Kim, M.-H.; Lee, S.Y.; Mehendale, S.S.; Webb, R.L. Microchannel Heat Exchanger Design for Evaporator and Condenser Applications. *Adv. Heat Transf.* **2003**, *37*, 297–429.
4. Lin, L.; Kedzierski, M. Review of low-GWP refrigerant pool boiling heat transfer on enhanced surfaces. *Int. J. Heat Mass Tran.* **2019**, *131*, 1279–1303. [CrossRef]
5. Kim, M.-H.; Shin, J.S. Evaporating heat transfer of R22 and R410A in horizontal smooth and microfin tubes. *Int. J. Refrig.* **2005**, *28*, 940–948. [CrossRef]
6. Kim, M.-H.; Shin, J.S. Condensation heat transfer of R22 and R410A in horizontal smooth and microfin tubes. *Int. J. Refrig.* **2005**, *28*, 949–957. [CrossRef]
7. Mota-Babiloni, A.; Makhnatch, P.; Khodabandeh, R.; Navarro-Esbrí, J. Experimental assessment of R134a and its lower GWP alternative R513A. *Int. J. Refrig.* **2017**, *74*, 682–688. [CrossRef]
8. Wang, C.-C. An overview for the heat transfer performance of HFO-1234yf. *Renew. Sustain. Energy Rev.* **2013**, *19*, 444–453. [CrossRef]
9. Aprea, C.; Greco, A.; Maiorino, A. HFOs and their binary mixtures with HFC134a working as drop-in refrigerant in a household refrigerator: Energy analysis and environmental impact assessment. *Appl. Therm. Eng.* **2018**, *141*, 226–233. [CrossRef]

10. Yıldız, A.; Yıldırım, R. Investigation of using R134a, R1234yf and R513A as refrigerant in a heat pump. *Int. J. Environ. Sci. Technol.* **2021**, *18*, 1201–1210. [CrossRef]
11. Lemmon, E.W.; Bell, I.H.; Huber, M.L.; McLinden, M.O. *NIST Standard Reference Database 23: Reference Fluid Thermodynamic and Transport Properties-REFPROP, Version 10.0, National Institute of Standards and Technology*; Standard Reference Data Program: Gaithersburg, MD, USA, 2018.
12. Zhao, C.-Y.; Ji, W.-T.; Jin, P.-H.; Zhong, Y.-J.; Tao, W.-Q. The influence of surface structure and thermal conductivity of the tube on the condensation heat transfer of R134a and R404A over single horizontal enhanced tubes. *Appl. Therm. Eng.* **2017**, *125*, 1114–1122. [CrossRef]
13. Ji, W.-T.; Chong, G.-H.; Zhao, C.-Y.; Zhang, H.; Tao, W.-Q. Condensation heat transfer of R134a, R1234ze(E) and R290 on horizontal plain and enhanced titanium tubes. *Int. J. Refrig.* **2018**, *93*, 259–268. [CrossRef]
14. Diani, A.; Cavallini, A.; Rossetto, L. R1234yf flow boiling heat transfer inside a 2.4-mm microfin tube. *Heat Tran. Eng.* **2017**, *38*, 303–312. [CrossRef]
15. Diani, A.; Campanale, M.; Cavallini, A.; Rossetto, L. Low GWP refrigerants condensation inside a 2.4 mm ID microfin tube. *Int. J. Heat Mass Tran.* **2018**, *86*, 312–321. [CrossRef]
16. Diani, A.; Cavallini, A.; Rossetto, L. R1234yf condensation inside a 3.4 mm ID microfin tube. *Int. J. Refrig.* **2017**, *75*, 178–189. [CrossRef]
17. Longo, G.A.; Zilio, C. Condensation of the low GWP refrigerant HFC1234yf inside a brazed plate heat exchanger. *Int. J. Refrig.* **2013**, *36*, 612–621. [CrossRef]
18. Yang, C.-Y.; Nalbandian, H. Condensation heat transfer and pressure drop of refrigerants HFO-1234yf and HFC-134a in small circular tube. *Int. J. Heat Mass Tran.* **2018**, *127*, 218–227. [CrossRef]
19. Li, H.; Hrnjak, P. Heat Transfer Coefficient, Pressure Gradient, and Flow Patterns of R1234yf Evaporating in Microchannel Tube. *ASME J. Heat Transf.* **2021**, *143*, 042501. [CrossRef]
20. Kedzierski, M.; Goncalves, J.M. Horizontal convective condensation of alternative refrigerants within a micro-fin tube. *J. Enhanc. Heat Transf.* **1999**, *6*, 161–178. [CrossRef]
21. Diani, A.; Campanale, M.; Rossetto, L. Experimental study on heat transfer condensation of R1234ze(E) and R134a inside a 4.0 mm OD microfin tube. *Int. J. Heat Mass Tranf.* **2018**, *126*, 1316–1325. [CrossRef]
22. Diani, A.; Rossetto, L. R513A flow boiling heat transfer inside horizontal smooth tube and microfin tube. *Int. J. Refrig.* **2019**, *107*, 301–314. [CrossRef]
23. Diani, A.; Brunello, P.; Rossetto, L. R513A condensation heat transfer inside tubes: Microfin tube vs. smooth tube. *Int. J. Heat Mass Tran.* **2020**, *152*, 119472. [CrossRef]
24. Karageorgis, A.; Hinopoulos, G.; Kim, M.-H. Condensation heat transfer and pressure drop characteristics of R513A as an alternative of R134a. In Proceedings of the 13th IEA Heat Pump Conference, Jeju, Korea, 26–29 April 2021.
25. Moffat, J. Describing the uncertainties in experimental results. *Exp. Therm. Fluid Sci.* **1998**, *1*, 3–17. [CrossRef]